Volume 9 | Number 1 | 7 January 2017 | Pages 1–178

Analytical Methods

rsc.li/methods

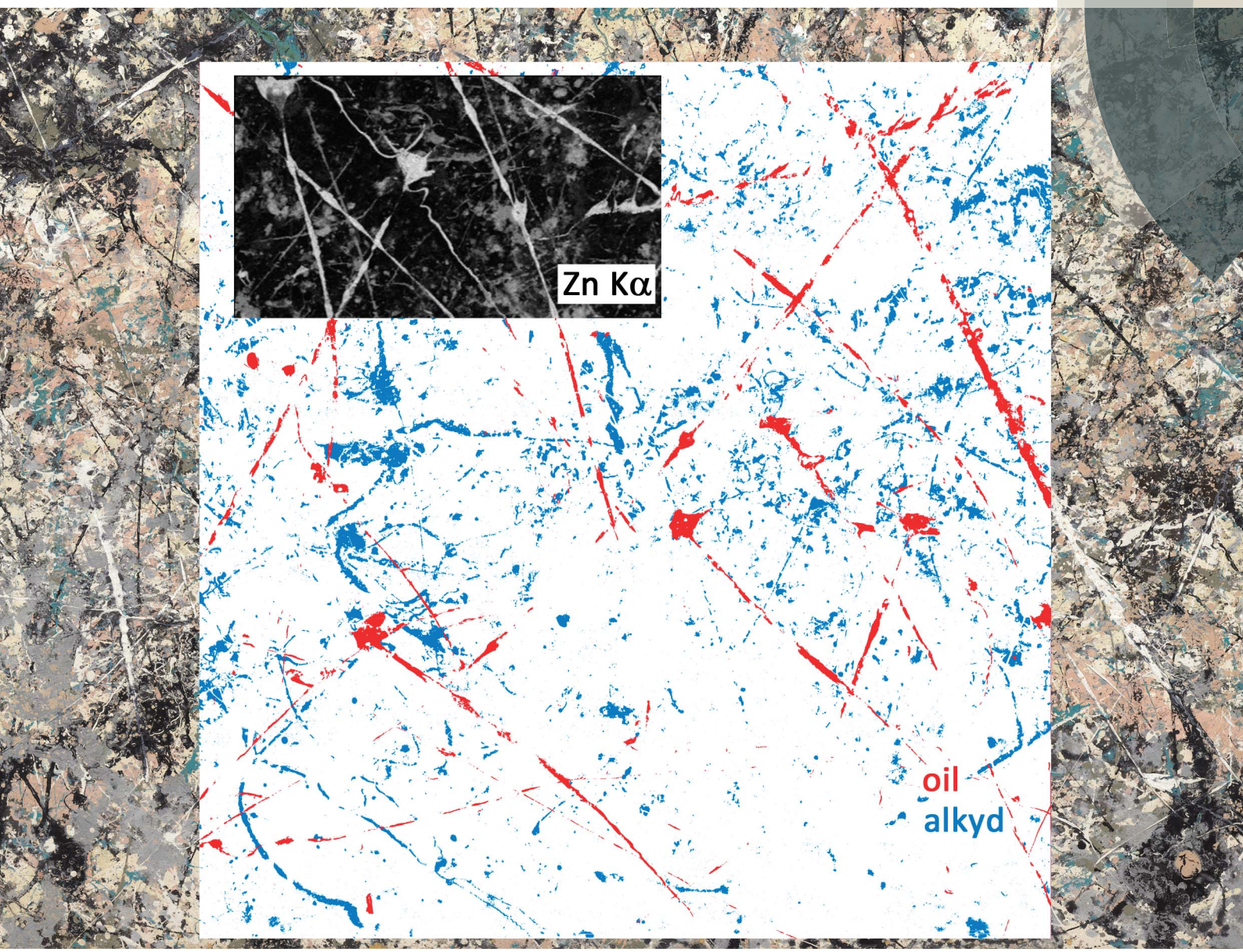

ISSN 1759-9679

ROYAL SOCIETY OF CHEMISTRY

PAPER

Kathryn A. Dooley *et al.*

Standoff chemical imaging finds evidence for Jackson Pollock's selective use of alkyd and oil binding media in a famous 'drip' painting

Analytical Methods

PAPER

View Article Online
View Journal | View Issue

Cite this: *Anal. Methods*, 2017, **9**, 28

Standoff chemical imaging finds evidence for Jackson Pollock's selective use of alkyd and oil binding media in a famous 'drip' painting

Kathryn A. Dooley,[ab] James Coddington,[c] Jay Krueger,[d] Damon M. Conover,[ab] Murray Loew[b] and John K. Delaney*[ab]

Received 24th June 2016
Accepted 20th September 2016

DOI: 10.1039/c6ay01795a

www.rsc.org/methods

Near-infrared diffuse reflectance imaging spectroscopy (NIR-RIS, 1000 to 2500 nm) was used to map the use of alkyd and oil paints in Jackson Pollock's *Number 1, 1950* (*Lavender Mist*), one of his most important 'drip' or 'poured' paintings. Pollock's drip paintings were created by allowing the paint to "pour" from his brush/stick down onto the canvas. Prior analysis of micro-samples from drip paintings found Pollock was extensively using alkyd-resin paints by 1949 (in addition to oil) which led to a hypothesis that he selectively used alkyd and oil paints to obtain the fluid, gestural marks characteristic of his mature style. To determine where he used alkyd and oil paints in *Lavender Mist*, we utilized near-infrared spectral regions (1615–1850 and 1860–2200 nm) that allowed discrimination between these binding media, especially when the first derivative spectra were examined. The near-infrared image cubes were collected with a high-spectral resolution (2.8 nm sampling) hyperspectral camera. Using convex geometry-based multivariate analysis, three spectral endmembers were identified: oil, alkyd resin, and a third binder. The mapping results show oil binding medium was confined to the uppermost layers of the painting, corresponding with long, more-or-less straight, white skeins of paint. An alkyd binding medium maps to long white skeins of paint (both straight and curved), in addition to many irregular-shaped, disconnected regions of white and blue-green paint, indicating the mapped alkyd paint is below other layers. The third spectral endmember maps to an off-white paint that may be a mixture/layering of oil and alkyd media. X-Ray fluorescence imaging spectroscopy and site-specific reflectance spectroscopy (350–2500 nm) found evidence that the oil and alkyd white paints contain zinc and titanium whites. However, the oil paint likely contains the anatase mineral form of titanium dioxide, whereas the alkyd paint likely contains rutile titanium dioxide. As these pigments do not absorb near-infrared radiation, the mapping results demonstrate the ability to use NIR-RIS to map modern paint binders. Furthermore, the use of oil and alkyd paints seem to be intentional choices by Pollock: the oil because it has more body, and the alkyd because it is more fluid and dries more quickly.

1 Introduction

The development of standoff chemical imaging techniques of fine art objects on the macroscale initially began with diffuse reflectance imaging spectroscopy (RIS). The goal of early studies was to demonstrate the feasibility of applying RIS to works of art by showing useful spectral information or new spatial information could be obtained.[1–4] Subsequent studies using more sophisticated analysis algorithms and larger spectral ranges demonstrated robust mapping of artists' materials by RIS was possible.[5,6] Techniques now routinely used include visible and near-infrared RIS[7] and the more recently developed X-ray fluorescence imaging spectroscopy (mXRF).[8]

Visible and near-infrared RIS provide information about molecular composition and structure based on electronic and vibrational transitions, whereas mXRF provides elemental information based on atomic transitions. Both reflectance and XRF imaging spectroscopy techniques have proven useful in revealing painted compositions below the artwork surface[9] and identifying and mapping the spatial distribution of pigments within paintings and illuminated manuscripts.[10] Like *in situ* reflectance and XRF point analysis methods, a more complete understanding is obtained when these imaging methods are applied in tandem and the results analysed together. We have previously demonstrated this by comparing the results of RIS

[a]*Scientific Research Department, National Gallery of Art, 4th and Constitution Ave NW, Washington, D.C. 20565, USA. E-mail: j-delaney@nga.gov*
[b]*School of Engineering and Applied Science, George Washington University, 800 22nd St NW, Science & Engineering Hall, Washington, D.C. 20052, USA*
[c]*Paintings Conservation Department, Museum of Modern Art, 11 W 53rd St, New York, NY, 10019, USA*
[d]*Paintings Conservation Department, National Gallery of Art, 4th and Constitution Ave NW, Washington, D.C. 20565, USA*

(400 to 1680 nm) and mXRF to identify and map the spatial distribution of original pigments, non-original inpaint, and underdrawing in an Early Renaissance panel painting of the Virgin Mary by Cosimo Tura.[6]

While pigments play an important role in gaining insight into the traditional working methods of artists, the study of the use of paint binders is no less important. Early treatises on painting methods suggest particular binders be used with specific pigments.[11] In Old Master paintings, prior to the widespread use of drying oils, some artists selectively used animal skin binders for blue pigments like azurite and natural ultramarine, and egg yolk tempera for reds, yellows, and lead white.[12] The reasoning behind these recommendations is thought to be the yellow color of egg yolk could make the blue passages appear greenish, and the higher refractive index of egg yolk would make the lead white more opaque. Thus, being able to non-invasively characterize the binding media can provide insight into an artist's working methods and connect their practice to written formulas.

When RIS data collection is extended into the near-infrared (NIR) to 2400 nm, the ability to separate and map paint binding media, such as egg yolk tempera, animal skin glue, wax, starch, and gums, in Old Master paintings can be achieved. The first use of near-infrared RIS to selectively map paint binders was demonstrated on an illuminated manuscript cutting attributed to Lorenzo Monaco.[13] The maps reveal the central figure was executed in egg yolk tempera, an unusual choice for an illuminator in the 15th century, but not necessarily for Monaco, who was a panel painter accustomed to painting with egg yolk tempera. The mapping of multiple binding media (egg yolk tempera and animal skin glue) has been performed on the previously mentioned panel paintings by Cosimo Tura, where prior micro-sampling had verified the presence of these binders by HPLC analysis.[14]

Binding media plays a large role in modern 20th century paintings. Improved drying oils, alkyd resins, and acrylics, for example, offer different viscosities, drying properties, and optical properties that can be exploited by the artist. Mixing or layering of different binders can create unique optical effects, such as those seen in the works by Arthur Dove,[15] Willem de Kooning,[16] and Mark Rothko.[17] An ideal candidate to explore the utility of RIS to map spatially varying binding media is Jackson Pollock, considered one of the most important artists in the twentieth century and a pioneer in the Abstract Expressionism movement.[18,19] Specifically, his 'drip' or 'poured' paintings were a style he developed and evolved in the 1940's. Pollock famously did not brush the paint in these works, choosing instead to dip his brush/stick into the paint can and "pour" the paint down onto the canvas. This resulted in the unique fluid, gestural marks that define his mature style of the late 1940's and early 1950's.

Evidence suggesting Pollock's drip paintings are a good test case comes from the FTIR and GC-MS analysis of samples taken from nine Pollock drip and poured paintings from 1943–1950 which found drying oil, oleoresinous, and alkyd-based paints.[20] Traditional oil media contain lipid triglyceride molecules that chemically dry through oxidative cross-links that form between side chains of the fatty acids. An alkyd is an ester formed from a polyhydric alcohol (or its anhydride) and a polybasic acid. Alkyds can be modified through the incorporation of drying oil fatty acids, subsequently known as oil-modified alkyd polyesters or alkyd resins. First developed in the late 1910's,[21] alkyd resins have a shorter drying time than traditional oil paints. Alkyd resins first dry by solvent evaporation and form a tack-free film more quickly than oil because the larger aromatic ring/aliphatic chain ratio makes the film more rigid and increases the glass transition temperature of the polymer.[22] Drying then proceeds by an auto-oxidation cross-linking reaction as in oil paints. The higher molecular weight of alkyd resins (due to larger aromatic ring/aliphatic chain ratio) also serves to reduce (as compared to a traditional oil) the number of cross-links needed to form a coherent film.[23] The development of new materials like alkyd resins was essential for the evolution of Pollock's technique.[24]

In this paper, absorption features in the NIR (1600–2500 nm) that arise from differences between binding media are used to identify and spatially map the location of oil and alkyd binders in one of Pollock's most important drip paintings, *Number 1, 1950* (*Lavender Mist*). *Lavender Mist* was painted in 1950, and is in the collection of the National Gallery of Art, DC. Site-specific reflectance spectroscopy and mXRF were also used to map and infer the pigments associated with each binder.

2 Experimental methods

2.1 Reflectance imaging spectroscopy (RIS) and data analysis

Diffuse reflectance image cubes were collected with a novel, high-spectral resolution, high-sensitivity, near-infrared, hyperspectral camera. The camera consists of a fore optic, a transmission grating imaging spectrometer (N25E, Specim Corp., Finland), relay optic, and a cryo-cooled 1280 × 1024 pixel InSb detector array (model IRC912, IRCameras, Santa Barbara, CA) which is band-pass limited to near-infrared light and has a 100% cold stop efficiency. The hyperspectral camera is sensitive from 1000–2500 nm with a small spectral sampling of ~2.8 nm and with a signal to noise greater than 300 : 1. Both are required to be able to spectrally distinguish among many paint binders because of their narrow spectral features (<15 nm) and small amplitudes. The camera allows for simultaneous collection of 1024 spectra along the slit.

The painting was diffusely illuminated with four lamps fitted with a 125 W halogen bulb and a light scattering plate. The lamps were placed in pairs on both sides of the detector at approximately 45 degrees from the painting normal. The light intensity levels could be varied with a rheostat and the light levels and integration time were adjusted so ~60% of the detector's dynamic range was used when imaging a gray Spectralon standard (50% diffuse reflector, Labsphere Inc., North Sutton, NH). This illumination configuration provided ~770 lux at the surface of the artwork. The recommended maximum light level for conservation photography of polychrome works of art like in this study is 2000–2500 lux when using non-flash, incandescent sources.[25,26] Thus, illuminating with 770 lux, which is close to typical office lighting conditions (~500 lux), is

reasonable. Using an integration time of 125 ms, hyperspectral reflectance images were acquired from an approximate 1 × 1 m area by using a high-precision, 2-axis easel (SmartDrive, Cambridge, UK) to move the painting in front of the stationary lights and detector for a total acquisition time of approximately 1 hour. The spatial sampling at the artwork was 0.248 mm per pixel.

2.2 Image processing of reflectance image cubes

The image cubes were flat-fielded using the gray Spectralon standard (50% diffuse reflector, Labsphere Inc., North Sutton, NH) and a "dark" cube collected with the camera shuttered. These gray and "dark" image cubes are used to correct for pixel-to-pixel response variation in the detector and non-uniformity in the illumination. Small black and white Spectralon standards (2% and 99% diffuse reflectors) included in the scene are used to calibrate all spectra to apparent diffuse reflectance *via* the empirical calibration tool in ENVI image analysis software (ENVI 5.0, Exelis VIS, Boulder, CO).

The image cubes were aligned spatially, or registered, to a reference color image using the registration algorithm described in Conover *et al.*[27] Once registered, the reflectance spectra were smoothed with a rolling average filter (width = 5 channels), and the first derivative with respect to wavelength was calculated. The first derivative is the slope of the reflectance with respect to wavelength. Absorption features in reflectance spectra give rise to a change in slope, and even a weak, narrow absorption feature or an absorption shoulder can result in sharp changes in slope. On the other hand, slowly varying changes in reflectance have little-to-no sudden changes in slope, and thus large baseline or offset differences (as seen between spectra of some pigments and ground layers) are effectively de-emphasized in the first derivative. Thus, first derivative spectroscopy is an effective way to distinguish between oil and alkyd resin reflectance spectra in the NIR because differences in baselines are minimized and small differences in narrow absorption features are accentuated. Using ENVI image analysis software and algorithms previously described,[5,10] data analysis of the first derivative cubes was performed on spectral subsets whose wavelength regions encompassed the greatest spectral differences between the binding media of interest. The best spectral subsets for separating and mapping alkyd and oil were 1615–1850 nm and 1860–2200 nm, respectively. For each spectral subset, the minimum noise fraction transform in ENVI was used to perform principal component analysis on whitened data (the data points are transformed such that their variance is uniform in the multidimensional space), yielding eigenimages or principal component (PC) images. The first 10 out of 125 (analysis of oil) or 12 out of 85 (analysis of alkyd) PC images were kept, as the remaining ones had low eigenvalues, describing mainly noise and having little-to-no image content related to the painting. A plot of the eigenvalues *versus* PC image number shows the eigenvalues decrease rapidly, followed by a slow asymptotic approach to zero. The PC threshold is determined by choosing the PC image with the lowest eigenvalue that still contains spatial image content. Next, a convex geometry algorithm known as the pixel purity index was used to find a subset of pixels in the hyperspectral cube whose spectra are the most unique and diverse. These pixels are then clustered in the reduced multidimensional space defined by the number of PC images that were retained. The *n*-D Visualizer in ENVI allows the user to visualize which pixels are well separated into clusters. The average spectra of selected clusters form a basis set of spectra, known as spectral endmembers, which describe the components in the image.

The endmember spectra are compared with spectral databases to identify the components present. Subtle spectral differences can result in multiple endmember spectra being found for the same general class of binding media (*i.e.* oil or alkyd). For both oil and alkyd, 2 endmembers were found that well-described the distribution of each medium in the image. These subtle spectral differences may arise from slight differences in composition (*e.g.* possibly different types/lengths of drying oil) or spatial differences in illumination conditions and collection geometry. The endmember spectra can then be used to make false-color maps using the spectral angle mapping algorithm which identifies pixels in the hyperspectral cube whose first derivative spectra match the endmember spectra within a specified tolerance angle. In the resulting maps, two endmember spectra representing oil and two for alkyd have been combined to show the spatial distribution of oil or alkyd, respectively.

2.3 Fiber-optic reflectance spectroscopy (FORS)

Reflectance spectra were collected at various sites on the painting with a portable, fiber-optic spectroradiometer (FieldSpec-3, ASD Inc., Boulder, CO) which operates from 350–2500 nm. The illumination source is a probe (A122317, ASD Inc.) held ~10 cm from the surface. The illumination light (~5000 lux) is incident on the surface only during data collection so as to minimize light exposure. The collection spot size at the surface is ~3 mm in diameter, and the acquisition time is 6 s per spectrum (64 averages).

2.4 X-Ray fluorescence imaging spectroscopy (mXRF) and data analysis

X-Ray fluorescence imaging spectroscopy was completed with a system designed in-house. The X-ray source is a rhodium tube operating at 50 kV and 500 μA (ARTAX, Bruker AXS Inc.) and fitted with 60 μm polycapillary collimating optics. A silicon drift detector (Vortex-90EX, Hitachi High-Technologies Science America, Inc.) operates at a peaking time of 0.5 μs and 13.7 eV sampling. A 0.3 × 0.5 m area of the painting was scanned using a high-precision, 2-axis easel (SmartDrive, Cambridge, UK). The spatial sampling was 1 mm, and the integration time was 100 ms, for a total acquisition time of approximately 4.2 hours. The XRF spectra were smoothed with a rolling average filter that was 68.5 eV wide (width of 5 spectral channels), and then registered to a reference color image.[27] Element maps of spatial distribution were generated by plotting the intensity at a single, characteristic energy value for each element.

3 Results and discussion

3.1 Reference NIR reflectance and first derivative spectra of oil and alkyd binding media

A reference NIR spectrum of cold-pressed linseed oil is shown in Fig. 1a, along with the structure of a representative triglyceride found in linseed oil, derived from linoleic, α-linolenic, and oleic acid. The distinguishing NIR spectral features of an oil are from the lipid triglyceride molecules in the oil and the majority of bands have been previously assigned by Vagnini *et al.*[28] The most characteristic absorptions include a combination band of antisymmetric/symmetric stretching and bending ($\nu + \delta$) of the methylenic (CH_2) groups that presents itself as a doublet near 2303 and 2346 nm, respectively, and the first overtone (2ν) of CH_2 stretching that occurs as a doublet near 1723 and 1755 nm. Other band assignments are shown in Table 1.

A reference NIR spectrum of an alkyd resin, along with a representative structure is also shown in Fig. 1a (see blue spectrum). Because fatty acids are a component of the alkyd resin, their NIR spectra share many of the same spectral features of a traditional drying oil. The same CH_2 combination and overtone bands can be seen, and the reference spectra of linseed oil and alkyd resin displayed no appreciable wavelength shift of these absorptions.

However, spectral differences do arise due to the aromatic component of the alkyd resins. More prominent shoulders near 1675 and 2265 nm appear at the lower wavelength side of the CH_2 absorption doublets, assigned as the first stretching overtone of aromatic C–H and possibly a combination stretching and bending of the aromatic C–H groups, respectively.[29] These shoulders are accentuated in the first derivative spectra, shown in Fig. 1b. For example, the shaded spectral region from

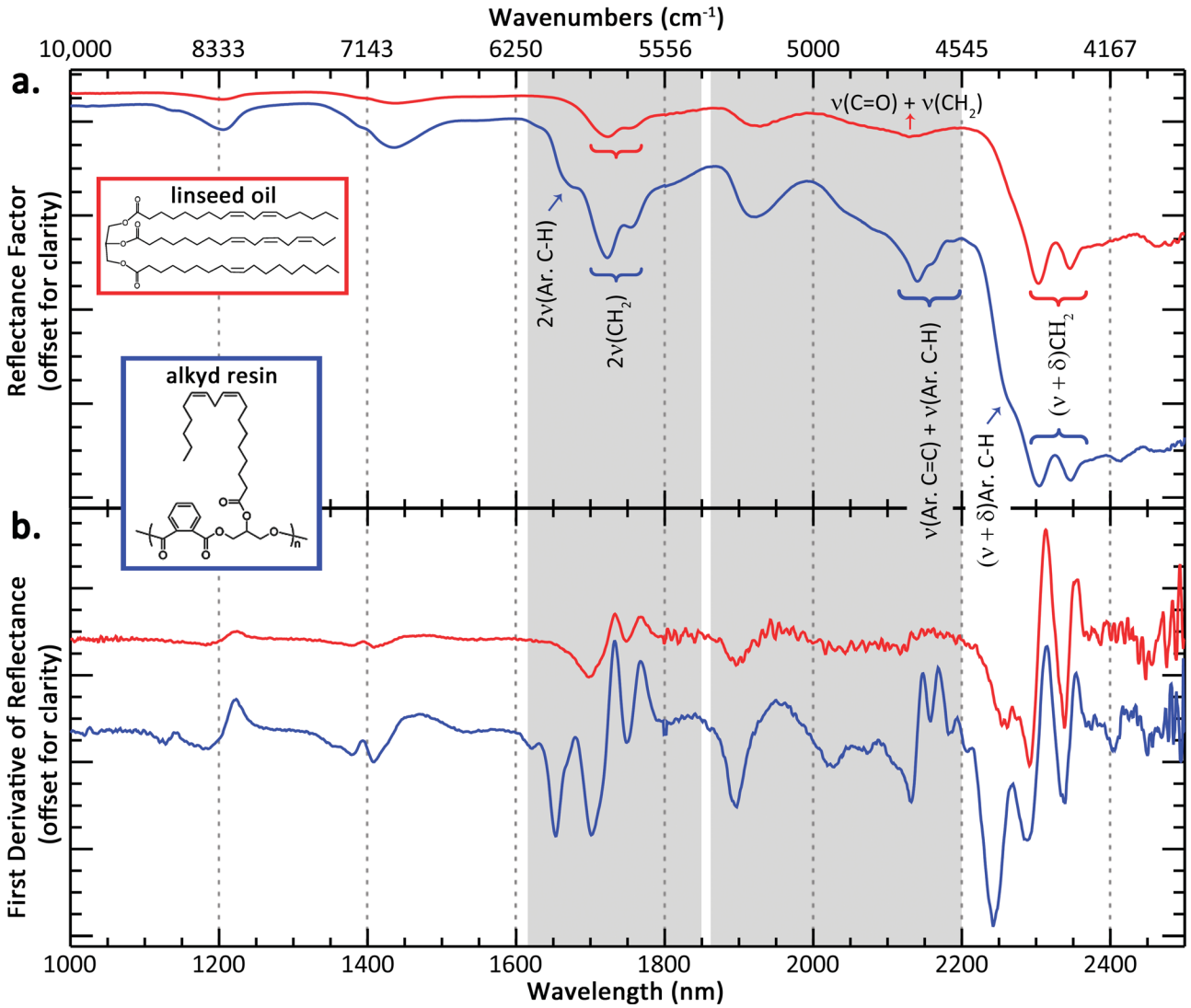

Fig. 1 (a) Reference reflectance spectra of cold-pressed raw linseed oil (Natural Pigments #510-41OCP, shown in red) and soy-based alkyd resin (sample from Robert Gamblin of Gamblin Artists Colors, shown in blue) on glass slides, measured in reflection on Spectralon 99% reflector standard. Relevant spectral features are labeled. (b) Corresponding first derivative spectra of the oil and alkyd reflectance spectra shown in (a). Differences between the media are most apparent in the spectral regions highlighted in gray from 1615–1850 nm and 1860–2200 nm, and these regions are used for media mapping.

Table 1 Tentative near-infrared band assignments of oil and alkyd resin binding media. A white background denotes spectral features that appear in both oil and alkyd spectra, and a blue background indicates features present in spectra of alkyd resins

nm	cm^{-1}	Band assignment
1138	8787	3ν(Ar. CH)
1204	8306	$3\nu(CH_2)$
1391	7189	$2\nu(CH_3) + \delta(CH_3)$
1434	6974	$2\nu(CH_2) + \delta(CH_2)$
1674	5974	2ν(Ar. CH)
1723	5804	$2\nu_{asym}(CH_2)$
1755	5698	$2\nu_{sym}(CH_2)$
1922	5203	$3\nu(C{=}O)_{aliphatic/aromatic\ ester}$
2132	4690	$\nu(C{=}O) + \nu(CH_2)$
2141	4671	ν(Ar. CH) + ν(Ar. C=C); $\nu(C{=}O) + \nu(CH_2)$
2161	4627	ν(Ar. CH) + ν(Ar. C=C)
2190	4566	ν(Ar. CH) + ν(Ar. C=C)
2262	4421	ν(Ar. CH) + δ(Ar. CH); $\nu(CH_3) + \delta(CH_3)$
2303	4342	$\nu_{asym}(CH_2) + \delta(CH_2)$
2346	4263	$\nu_{sym}(CH_2) + \delta(CH_2)$
2413	4144	$\nu(CH_2) + \nu(C{-}CO{-}O)_{aromatic\ ester}$
2460–2485	4065–4024	$\nu(CH_2) + \nu(C{-}CO{-}O)_{aliphatic\ ester}$

1615–1850 nm contains the absorption due to the 2ν(Ar. C–H) that appears as a shoulder near 1675 nm in the alkyd reflectance spectrum, but this absorption feature results in a more distinct "peak" in the alkyd derivative spectrum. Another difference is the absorptions at 2140 nm and 2160 nm. As can be seen in Fig. 1a, the reference oil spectrum has an absorption centered near 2132 nm, assigned to a combination band of $\nu(C{=}O) + \nu(CH_2)$, and this combination band likely contributes to the absorptions centered at 2140 nm and 2160 nm seen in the alkyd spectrum. However, the greater intensity and different spectral shape in the alkyd spectrum likely has some contribution from a combination band of aromatic C=C and aromatic C–H ring stretches. This combination band is seen in other aromatic-containing polymers, such as polystyrene[30] and aromatic esters like polyethylene terephthalate.[31] Again, the differences between the oil and alkyd media are more apparent when looking at the derivative spectra from 1850–2200 nm (region highlighted in gray in Fig. 1b).

The broad feature between 2460–2480 nm is present in both oil and alkyd spectra and is possibly a combination band or a coupling of vibrational modes associated with CH_2 stretching and C–C(O)–O stretching of the aliphatic ester, based on mid-IR band assignments.[32,33] An analogous absorption occurs for the aromatic ester, and is seen in only the alkyd spectrum near 2415 nm.

Because of similarities in oil and alkyd spectra, in order to identify an alkyd, both the features characteristic of a drying oil but also at least the presence of the aromatic C–H overtone at ~1675 nm and aromatic C=C and C–H combination band at ~2140 nm need to be present. A paper by Rosi *et al.* proposed some band assignments for modern paint binding media, including alkyd resins, from ~1667 nm through the mid-IR spectral region,[34] but to our knowledge, this is the first comprehensive band assignment of alkyd resins in the near-infrared spectral region (1000–2500 nm). The intensities of the aromatic overtones and combination bands in the alkyd resin spectra are stronger than what would be expected based on their mid-IR spectra. The lower absorption coefficient in the near-infrared allows for more diffuse scattering by the pigment particles, effectively resulting in a larger interrogation volume of the binding medium between the particles. This enhances the band depth of NIR absorption features from the binding medium.

3.2 NIR reflectance imaging spectroscopy of Jackson Pollock's *Lavender Mist* – mapping the binding media

Once reference spectra of known binding materials were collected, the goal was to use these band assignments to identify and map paint binding media in a modern painting. A square meter (see Fig. 2a) of Jackson Pollock's *Number 1, 1950* (*Lavender Mist*) (total size ~ 3 × 2.2 meters) was imaged using the hyperspectral reflectance imaging system from 1000–2500 nm.

The first derivative of the calibrated image cubes was calculated. Spectral data analysis of the first derivative (using hyperspectral convex geometry algorithms) was performed from 1615–1850 nm and 1860–2200 nm, and endmember spectra (two for alkyd medium, two for oil medium, respectively) were identified.

The endmember spectra associated with oil media map to the regions shown in Fig. 2b. In general, oil media maps to long skeins of white paint, including some 'tadpole' shapes, suggested previously to have been made by squeezing paint directly from an open tube or from a hole in the tube body.[20,24] The path of each skein can be seen clearly, even though the oil skeins are not fully connected in the map. This discontinuity is because parts of each skein have been covered with additional paint where the media could not be identified. This additional paint is often black, gray, or silver metallic paint and has too low of a reflectance or causes too much specular reflection to be a good match to the oil endmember spectra.

Some of the oil skeins have been manipulated – either by dragging, smearing, or perhaps by using a solvent to thin the paint and blow it with a fan to create a thinner paint layer along one edge of the skein. The horizontal skein in the upper fifth of the map has tendrils directed upwards that are suggestive of this. This map also provides some information on the layering structure of the painting. The pattern of oil paint can be seen clearly because of the fact that the long white skeins of oil paint are on top of most of the other paint layers. In many areas, the long skeins can be seen to cross over other areas of paint (see map detail in Fig. 3b or 4b).

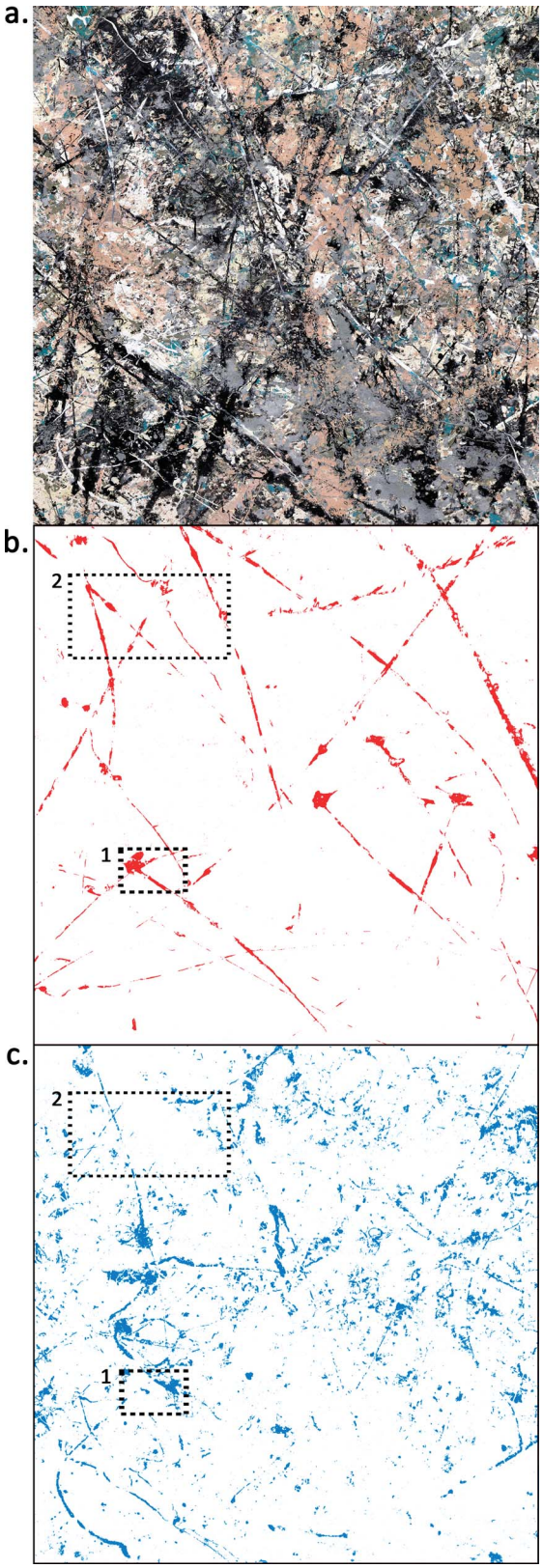

Fig. 2 (a) Color detail of ~1 × 1 m area of Jackson Pollock's *Number 1, 1950* (*Lavender Mist*). Ailsa Mellon Bruce Fund, 1976.37.1, National Gallery of Art, Washington, D.C. (b) False-color image showing the locations which map to the endmember derivative spectra representing oil and (c) alkyd. Media maps of areas denoted 1 and 2 are shown in Fig. 3 and 4, respectively.

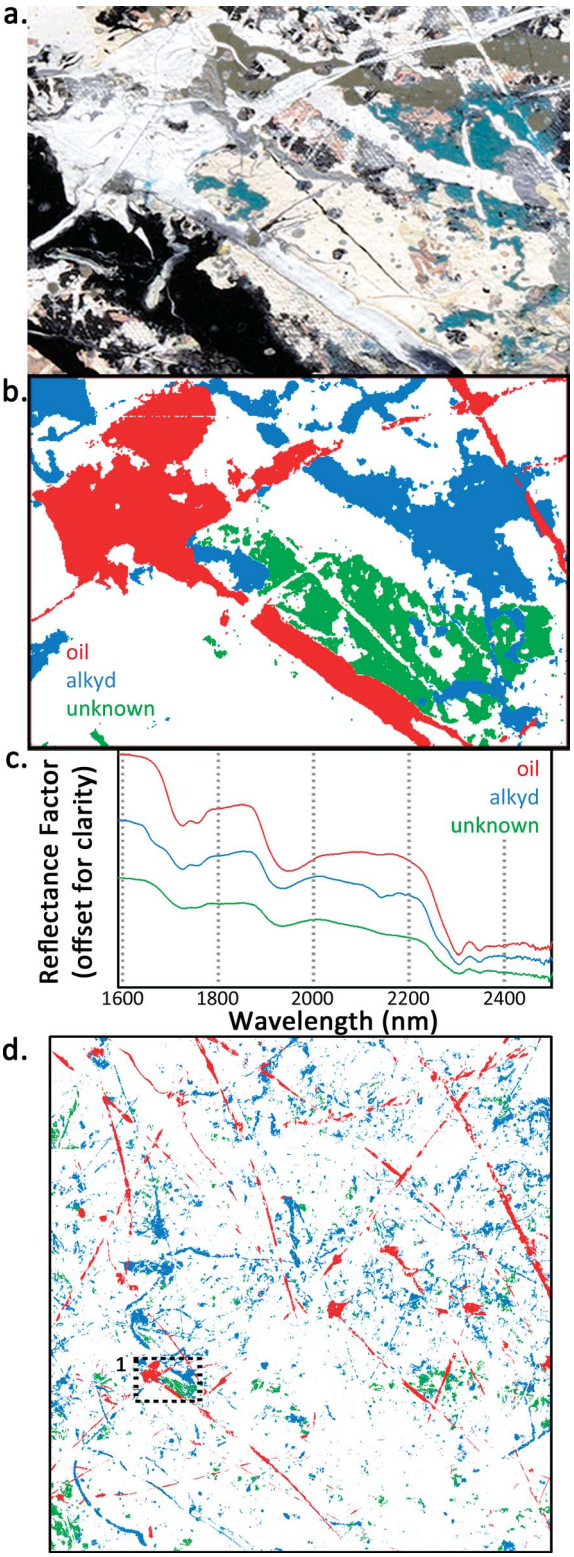

Fig. 3 (a) Color detail and (b) false-color image of detail #1 denoted with dashed lines in Fig. 2. Areas that map to the endmember derivative spectrum of oil, alkyd, and an unknown binder are shown in red, blue, and green, respectively. Both white and blue pigments map to the alkyd media. Where the media intersect, it can be seen that the unknown binder is below the alkyd, which in turn is below the oil. (c) FORS spectra from detail #1 region of the oil, alkyd, and unknown binder. (d) Overall media map of the ~1 m × 1 m area that was imaged.

The endmember spectra associated with alkyd media maps to the regions shown in Fig. 2c. These alkyd regions map to multiple pigments, including white and blue-green areas of the painting. Some lines in the alkyd map are similar in color and dimension to the long thin skeins of white paint that map to oil, suggesting that neither the color nor the scale and dimension of the paint lines is enough information to deduce the medium. Other mapped regions are curved lines (see lower left hand corner) that suggest a more fluid paint was possibly dripped from sticks or poured from a paint can. The layering over top of alkyd paint also can be inferred from Fig. 2c, which shows many small, irregular-shaped regions distributed throughout the scanned area. This is suggestive that much of the mapped alkyd paint was applied before other layers of paint. Its distribution appears more "broken up" because another paint with a different spectral signature resides on top. The regions appearing in the map are the alkyd paint that remains visible on the surface. This layering effect can also be seen in Fig. 3b and 4b where skeins of white oil paint (shown in red) sit on top of skeins of white alkyd paint (shown in blue) where the media intersect.

Fig. 3 shows the detail #1 region denoted with dashed lines in Fig. 2. Fig. 3a is the color image, and Fig. 3b is a false-color image with three binders mapped, including oil (red), alkyd (blue), and an unknown binder (green). The alkyd medium in this detail is associated with both white and blue paints, and an unknown medium maps to a yellow/cream-colored paint. FORS NIR reflectance spectra from the oil, alkyd, and unknown regions are shown in Fig. 3c. The green spectrum representing the unknown medium has spectral features similar to oil and alkyd and a slope similar to the alkyd paints from 2000–2200 nm. The absorption doublets near 1728/1755 and 2304/2348 nm (due to methylene groups in aliphatic chains) are broader by comparison with oil or alkyd spectra, which could suggest a mixture of fatty acids with slightly different compositions, resulting in a broadening of spectral features. The signal of the unknown medium could possibly be from a single layer that is a mixture of oil and alkyd media or the superposition of two or more layers comprised of oil and alkyd, respectively. The unknown medium could also be oleoresinous or associated with a locally applied varnish. Coddington describes sprayed passages in *Lavender Mist* (particularly visible under UV light) rich in varnish or a similar medium that were possibly used to provide tooth for subsequent applications of paint.[24] Perhaps the cream-colored regions are evidence of this practice.

This unknown medium is, in fact, below the other mapped paints as can be seen in the detail and the overall map in Fig. 3b and d. The unknown medium is below the alkyd paint where the media intersect, which is in turn below the oil paint. In this case, even though the medium denoted by the green regions cannot be conclusively determined with reflectance spectroscopy alone, its spatial distribution can still be mapped and information about the layering structure can be deduced.

Because black and metallic paint were used prominently throughout the composition and are associated with low reflectance values and specular reflection, it should be noted

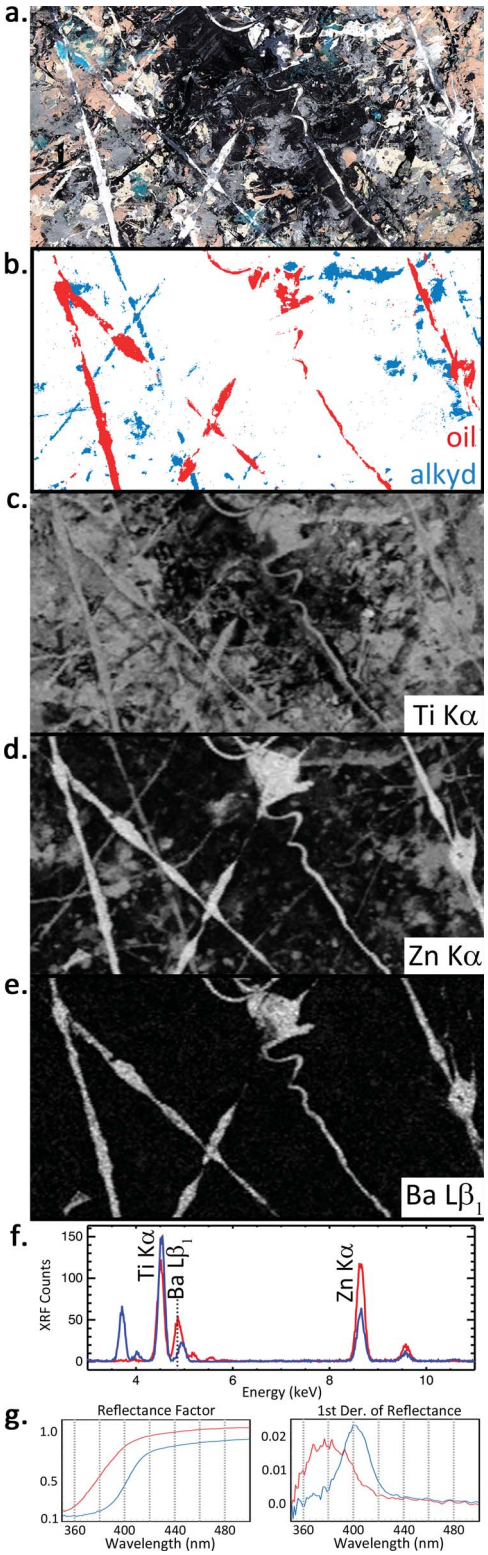

Fig. 4 (a) Color detail and (b) false-color image of detail #2 denoted with dashed lines in Fig. 2. Areas that map to the endmember derivative spectrum of oil and alkyd are shown in red and blue, respectively. The mapped binding media in this detail correspond to white paint. XRF element maps for (c) titanium, (d) zinc, and (e) barium are shown, along with (f) representative XRF spectra from a single pixel from the oil and alkyd regions. Reflectance and first derivative spectra are shown in (g), indicative of the difference in pigments between the two media.

that the medium of those paints cannot be identified with reflectance or first derivative spectroscopy.

It should also be noted that the first derivative analysis could be completed without spatial aggregation of the image cubes due to the high quality of individual spectra (spatial sampling at the artwork was 0.248 mm per pixel). This is useful because spatially aggregating the dataset (to increase the signal-to-noise ratio of the spectra) may have caused a mixing between areas of different media on *Lavender Mist*, a painting that consists of many spatially narrow features and drips/splatters of different paints throughout.

3.3 Pigment mapping and identification with mXRF and FORS

In addition to the media differences and order of application of oil and alkyd paints, the mapped regions also have different pigment composition. To aid in identification of the pigments, XRF imaging spectroscopy was completed in the region denoted as detail #2 in Fig. 2, and FORS measurements were also collected. Results are shown in Fig. 4. The reflectance spectra of the white oil paint show a transition edge at 378 nm with a full width at half maximum (FWHM) of ~43 nm (see Fig. 4g). Reference reflectance spectra of pure titanium dioxide (anatase form) and pure zinc oxide have transition edges at 372 nm (FWHM ~ 25 nm) and 384 nm (FWHM ~ 15 nm) respectively. The transition edge and comparatively wider FWHM in the oil paint is suggestive there may be a mixture of anatase titanium white and zinc white. The XRF mapping results are supportive of this conclusion, as both zinc and titanium, along with barium (exclusively in oil paint), were detected in the long white oil skeins (see Fig. 4c–e). Representative XRF spectra from the white oil and white alkyd paints are displayed in Fig. 4f. The FORS and XRF results provide evidence that the long skeins of white oil paint likely contain zinc and titanium whites. Because both zinc and titanium whites have high reflectance in the NIR, this ensures that the NIR spectral absorptions used for mapping the oil medium are not influenced by the pigments present.

Regarding the pigment in the white alkyd paint, the FORS spectra from this region have a transition edge at 401–404 nm with FWHM ~25 nm (Fig. 4g), which is characteristic of titanium dioxide in the rutile mineral form. Interestingly, this may suggest one mineral form of titanium dioxide is found in the alkyd medium (rutile) and another mineral form is found within the oil medium (anatase). This is possible as both anatase and rutile pigments were available in the US in the 1940's[35] but could be confirmed if samples of these paints were taken and analyzed with mid-IR or Raman spectroscopy, or X-ray diffraction. Both rutile and anatase forms of titanium white have been found in Pollock's 1949 painting *Number 10* at the Museum of Fine Arts in Boston[36] and also in paint cans from the Pollock-Krasner studio.[37]

XRF mapping does show that the alkyd white paint contains Ti, in addition to Zn and Ca with minor amounts of Fe and Pb. Hence, it is possible that the predominant pigments in the white alkyd paint are rutile titanium white with a smaller amount of zinc white and a calcium-containing filler, in contrast to a more evenly distributed mix of anatase titanium white and zinc white in the oil paint. The material differences between these two white paints also helps to explain the visual separation of these paints that has been observed under ultraviolet light.[24]

XRF spectra of the blue-green paint that mapped to an alkyd binder have an intense titanium peak, followed by Ca, then Zn, and smaller amounts of Pb and Fe. Traces of Cr are also detected in these areas. The FORS spectra of the blue-green paint have a weak transition edge at 394 (FWHM ~ 25 nm). The transition edge is lower than what would be expected for a pure rutile titanium dioxide (~404 nm), which could be due to a mixture of rutile with anatase titanium white and/or zinc white. The reflectance spectra also show a reflectance peak near ~500 nm, then a broad absorption centered near 710 nm with increasing reflectance from 800–1300 nm. These features are spectrally similar to reference spectra of Prussian blue. Thus, the pigments primarily responsible for the blue-green color are possibly due to a mixture of Prussian blue and a yellow such as lead or zinc chromate.

XRF spectra of the cream paints that mapped to an unknown binder show the presence of Ti and Ca, with trace amounts of Zn, Pb, and Fe. The FORS spectra of the cream pigments have a transition edge at 397 nm (FWHM ~ 25 nm). The lower transition edge relative to pure rutile titanium dioxide could be due to a mixture of rutile and anatase titanium whites.

4 Conclusion

Near-infrared reflectance imaging spectroscopy was applied to Jackson Pollock's *Lavender Mist* using a novel, high-spectral resolution and high-sensitivity hyperspectral camera. This NIR camera was key for enabling the collection of image cubes with sufficient spectral sampling and signal-to-noise such that small, narrow spectral features of the binding media could be distinguished and the first derivative image cube could be calculated and subsequently used to make robust maps of oil and alkyd binding media. The first derivative accentuates the subtle differences between the reflectance spectra of oil and alkyd binding media, and those media were more clearly separated in the first derivative than when analyzing the reflectance spectra. To our knowledge, this paper also presents the first comprehensive band assignment of near-infrared (1000–2500 nm) spectral features of alkyd resins.

The nature of this painting makes it difficult to visually identify areas of similar materials because the drips and splatters of color don't conform to a recognizable pattern. However, being able to separate materials based on chemical differences allowed for the creation of maps where each binding medium was isolated from the rest of the composition. The oil map, for example, allows the viewer to more easily visualize the campaign in which Pollock likely applied paint by squeezing an oil paint tube. In addition, a distinction could be seen between two white pigments that look visually similar but have different binding media, and between different pigments that have the same binding media.

Not only do the maps isolate areas with similar binding media composition, but they also provide information about

the layering structure of the painting. By comparing or overlaying the maps, some lines can be seen to reside on top of others where the media intersect. And in the alkyd map, the scattered distribution of the medium is suggestive that it resides below many other layers.

The use of point-based reflectance measurements (350–2500 nm) and X-ray fluorescence imaging spectroscopy helped to identify and map the pigments associated with the binding media. Titanium white (likely both the rutile and anatase mineral forms) and zinc white were found in the white oil and alkyd paints. Titanium white was also found in the cream areas that mapped to an unknown binding medium. The blue-green paint associated with an alkyd binder contained titanium white, Prussian blue, and likely a yellow such as lead or zinc chromate.

The identification of binding media and pigments in *Lavender Mist* contributes to the literature of the materials and techniques that Pollock used. The use of oil and alkyd paints were intentional choices by Pollock: the oil paint used because it has more body and provided a textural element, and the alkyd paint used because of its fluidity and quick drying nature. Pollock exploited their material and handling properties in order to achieve the specific and varied marks and gestures of this painting.

Acknowledgements

We thank Robert Gamblin of Gamblin Artists Colors for supplying a reference sample of alkyd resin. We thank Jennifer Hickey for help with FORS data collection and useful discussions about Pollock's technique, and Suzanne Lomax, Lisha Glinsman, and Kathryn Morales for helpful discussions regarding data interpretation. Dooley and Delaney acknowledge financial support from the National Science Foundation award 1041827 and the Andrew W. Mellon and Samuel H. Kress Foundations.

References

1 A. Casini, F. Lotti, M. Picollo, L. Stefani and E. Buzzegoli, *Stud. Conserv.*, 1999, **44**, 39–48.
2 J. R. Mansfield, M. G. Sowa, C. Majzels, C. Collins, E. Cloutis and H. H. Mantsch, *Vib. Spectrosc.*, 1999, **19**, 33–45.
3 D. A. K. Melessanaki, V. Papadakis and C. Balas, *Spectrochim. Acta, Part B*, 2001, **56**, 2337–2346.
4 M. Attas, E. Cloutis, C. Collins, D. Goltz, C. Majzels, J. R. Mansfield and H. H. Mantsch, *J. Cult. Heritage*, 2003, **4**, 127–136.
5 J. K. Delaney, J. G. Zeibel, M. Thoury, R. Littleton, M. Palmer, K. M. Morales, E. R. de la Rie and A. Hoenigswald, *Appl. Spectrosc.*, 2010, **64**, 584–594.
6 K. A. Dooley, D. M. Conover, L. D. Glinsman and J. K. Delaney, *Angew. Chem., Int. Ed.*, 2014, **53**, 13775–13779.
7 J. K. Delaney, M. Thoury, J. G. Zeibel, P. Ricciardi, K. M. Morales and K. A. Dooley, *Heritage Sci.*, 2016, **4**, 1–10.
8 M. Alfeld, J. V. Pedroso, M. van Eikema Hommes, G. Van der Snickt, G. Tauber, J. Blaas, M. Haschke, K. Erler, J. Dik and K. Janssens, *J. Anal. At. Spectrom.*, 2013, **28**, 760.
9 Y. Jackall, J. K. Delaney and M. Swicklik, *Burlingt. Mag.*, 2015, 248–254.
10 J. K. Delaney, P. Ricciardi, L. D. Glinsman, M. Facini, M. Thoury, M. Palmer and E. R. de la Rie, *Stud. Conserv.*, 2014, **59**, 91–101.
11 C. d'Andrea Cennini, *Il Libro dell' Arte*, Dover Publications, Inc., New York, 1960.
12 S. M. Halpine, *Stud. Conserv.*, 1992, **37**, 22–38.
13 P. Ricciardi, J. K. Delaney, M. Facini, J. G. Zeibel, M. Picollo, S. Lomax and M. Loew, *Angew. Chem., Int. Ed.*, 2012, **51**, 5607–5610.
14 K. A. Dooley, S. Lomax, J. G. Zeibel, C. Miliani, P. Ricciardi, A. Hoenigswald, M. Loew and J. K. Delaney, *Analyst*, 2013, **138**, 4838–4848.
15 R. Newman and I. Konefal, in *1993 AIC Paintings Specialty Group Postprints*, The American Institute for Conservation of Historic and Artistic Works, Washington, DC, 1993, pp. 81–85.
16 S. F. Lake, *Willem de Kooning: The Artist's Materials*, The Getty Conservation Institute, Los Angeles, 2010.
17 A. Langley and S. Q. Lomax, *Facture*, 2015, **2**, 110–137.
18 Y. Szafran, L. Rivers, A. Phenix, T. Learner, E. G. Landau and S. Martin, *Jackson Pollock's Mural: The Transitional Moment*, The J. Paul Getty Museum, Los Angeles, 2014.
19 *Jackson Pollock New Approaches*, ed. K. Varnedoe and P. Karmel, The Museum of Modern Art, New York, 1999.
20 S. Lake, E. Ordonez and M. Schilling, in *Modern Art, New Museums: IIC Contributions to the Bilbao Congress 2004*, 2004, pp. 137–141.
21 H. A. L. Standeven, *House Paints, 1900–1960: History and Use*, The Getty Conservation Institute, Los Angeles, 2011.
22 Z. W. Wicks Jr, F. N. Jones and S. P. Pappas, *Organic Coatings: Science and Technology*, John Wiley & Sons, Inc., New York, 1992.
23 R. Ploeger, *The Characterization and Stability of Artists' Alkyd Paints*, PhD Thesis, University of Torino, 2008.
24 J. Coddington, in *Jackson Pollock New Approaches*, ed. K. Varnedoe and P. Karmel, The Museum of Modern Art, New York, 1999, pp. 101–115.
25 G. Thomson, *The Museum Environment*, Butterworth-Heinemann Ltd., Oxford, 2nd edn, 1986.
26 F. Frey, D. Heller, D. Kushel, T. Vitale, J. Warda and G. Weaver, *The AIC Guide to Digital Photography and Conservation Documentation*, American Institute for Conservation of Historic and Artistic Works, Washington, D.C., 2008.
27 D. M. Conover, J. K. Delaney and M. H. Loew, *Appl. Phys. A: Mater. Sci. Process.*, 2015, **119**, 1567–1575.
28 M. Vagnini, C. Miliani, L. Cartechini, P. Rocchi, B. G. Brunetti and A. Sgamellotti, *Anal. Bioanal. Chem.*, 2009, **395**, 2107–2118.
29 J. Workman and L. Weyer, *Practical Guide to Interpretive Near-Infrared Spectroscopy*, Taylor & Francis Group, LLC, Boca Raton, 2007.
30 Y. Z. Ren, T. Murakami, T. Nishioka, K. Nakashima, I. Noda and Y. Ozaki, *J. Phys. Chem. B*, 2000, **104**, 679–690.

31 C. E. Miller and B. E. Eichinger, *Appl. Spectrosc.*, 1990, **44**, 496–504.
32 B. Smith, *Infrared Spectral Interpretation: A Systematic Approach*, CRC Press LLC, Boca Raton, 1999.
33 N. B. Colthup, L. H. Daly and S. E. Wiberley, *Introduction to Infrared and Raman Spectroscopy*, 1990.
34 F. Rosi, A. Daveri, P. Moretti, B. G. Brunetti and C. Miliani, *Microchem. J.*, 2016, **124**, 898–908.
35 M. Laver, in *Artists' Pigments: A Handbook of Their History and Characteristics*, ed. E. W. Fitzhugh, Oxford University Press, New York, 1997, vol. 3, pp. 295–355.
36 R. Newman and M. Derrick, in *Pollock Matters*, ed. E. G. Landau and C. Cernuschi, University of Chicago Press, Chicago, 2007, pp. 105–129.
37 N. Eastaugh and B. Gorsia, in *Pollock Matters*, ed. E. G. Landau and C. Cernuschi, University of Chicago Press, Chicago, 2007, pp. 143–153.